1.5. THE CONTROL OF ELECTRON TRANSFER DIRECTION AT THE ELECTRODES MODIFIED WITH SELF-ASSEMBLED MONOLAYERS

KOHEI UOSAKI

Physical Chemistry Laboratory, Division of Chemistry, Graduate School of Science, Hokkaido University, Sapporo 060, Japan

1.5.1 INTRODUCTION

In biological system, uni-directional electron transfer is achieved very effectively as functional molecules are arranged in order.[1] To mimic this system, it is essential to have a technique to arrange specific molecules on solid substrates in ordered manner so that electron transfer direction can be controlled.

A self-assembly (SA) technique has been very widely used to construct ordered molecular layers of various functionalities.[2] Molecular layers formed by the SA technique are expected to be more stable than those formed by the Langmuir-Blodgett (LB) method[3] because the interaction between the adsorbed molecules and substrate is chemisorption in the former but physisorption in the latter. Self-assembled monolayers (SAMs) of alkanethiols on metal electrodes have been the most well studied system. It is generally believed that alkanethiols form the SAMs as a result of the chemical bond formation between substrate atoms and sulfur atoms of thiols and the hydrophobic interaction between alkyl chains.[2] Thus, the SAM with an electrochemical active group formed on a gold and ITO electrode should be a good candidate for an uni-direction electron transfer system. Many investigations of electrodes modified with the SAM containing various electrochemical functionalities.[4–10] We have also studied the self-assembly process and the relation between the structure and functionalities of monolayers of alkanethiol derivatives with various functional groups such as ferrocene.[11–22]

Here we describe the electrochemical and/or photoelectrochemical characteristics of gold and/or ITO electrodes modified with the SAMs of various thiol molecules shown in Figure 1.5.1 as examples for the control of electron transfer direction.

1.5.2 UNI-DIRECTIONAL ELECTRON TRANSFER AT THE GOLD ELECTRODE MODIFIED WITH FERROCENYLALKANE THIOL (I) MONOLAYER[23]

Figure 1.5.2 shows cyclic voltammograms (CVs) of a ferrocenylundecanethiol ($FcC_{11}SH$, I) modified gold electrode in 1 M $HClO_4$ (a) and in 1 M $HClO_4$ solution containing 1 mM $Fe(ClO_4)_3$ at various sweep rate (b)–(e). As a comparison, CV at

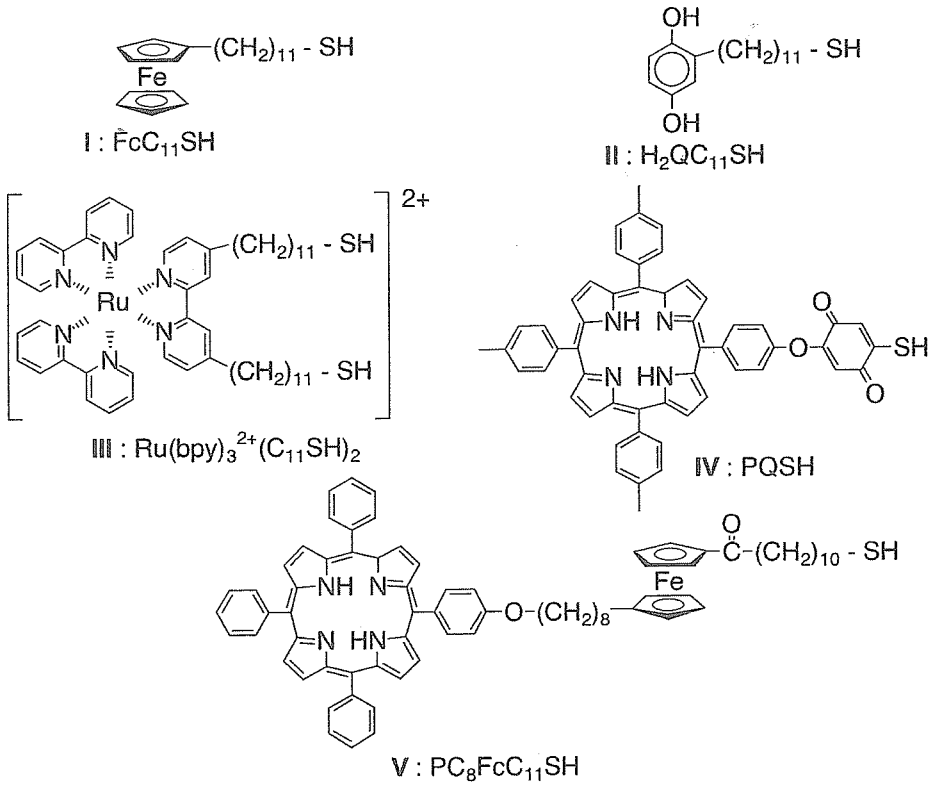

Figure 1.5.1. Molecules used in this section.

a bare gold electrode in 1 M $HClO_4$ + 1 mM $Fe(ClO_4)_3$ solution is also presented in Figure 1.5.2 (f). Although reversible redox peaks are observed in 1 M $HClO_4$ + 1 mM $Fe(ClO_4)_3$ solution at the bare gold electrode around +450 mV, reduction of Fe^{3+} is blocked at the $FcC_{11}SH$ modified gold electrode in this potential region. However, the cathodic peak current around +150 mV grows if $Fe(ClO_4)_3$ is present in solution. On the other hand, the anodic peak current at the same potential decreases by the addition of $Fe(ClO_4)_3$. The degree of increase of the cathodic peak current is larger when the sweep rate is lower. The electrochemical characteristics of the electrode is strongly affected by the concentration of $Fe(ClO_4)_3$ in solution. The cathodic peak current increases linearly with the concentration of $Fe(ClO_4)_3$ in solution.

These results can be explained as follows. Since the redox potential of Fe^{2+}/Fe^{3+} couple in solution is more positive than that of the surface-attached ferrocenyl group, once ferricenium cation site is reduced to ferrocene at +150 mV, the ferrocenyl group donates an electron to $Fe^{3+}{}_{aq}$. As a result, $Fe^{2+}{}_{aq}$ is formed and ferrocene becomes ferricenium cation which accepts an electron from the electrode and the

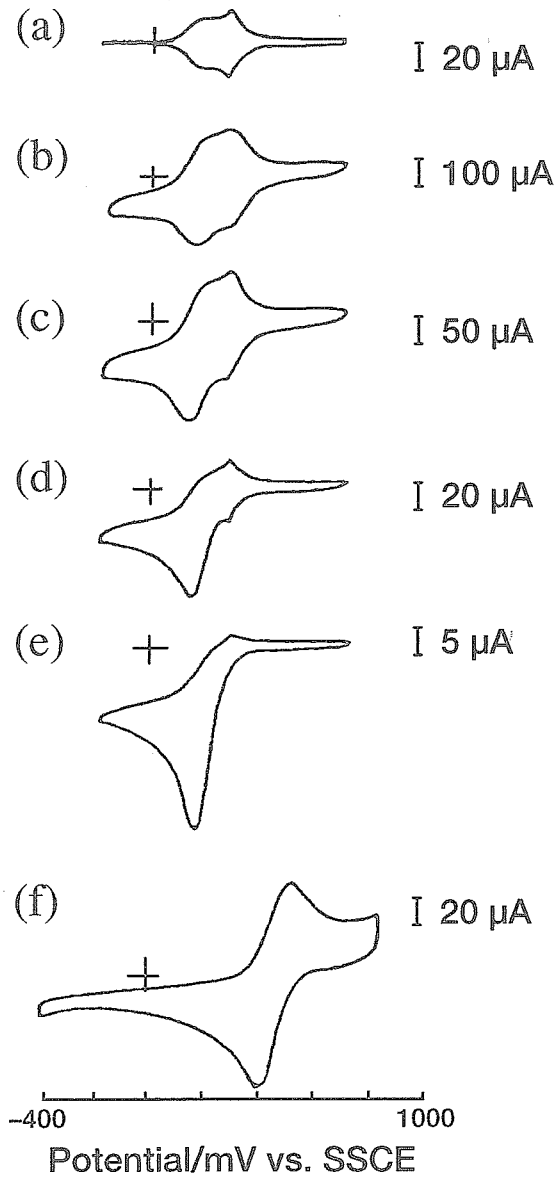

Figure 1.5.2. CVs of the gold electrode modified with the $FcC_{11}SH$ SAM measured in (a) 1 M $HClO_4$ with a scan rate of 100 mV/s and (b)-(e) 1 M $HClO_4$ containing 1 mM $Fe(ClO_4)_3$ with scan rate of (b) 1000 mV/s, (c) 500 mV/s, (d) 100 mV/s and (e) 10 mV/s. (f) CV of the bare gold electrode in 1 M $HClO_4$ containing 1 mM $Fe(ClO_4)_3$ with a scan rate of 100 mV/s.

surface ferrocene is regenerated as potential is more negative than the redox potential of ferrocenyl group. These steps are repeated and a large cathodic current flows, as summarized in the following Scheme 1.5.1.

Scheme 1.5.1.

In other words, surface ferrocenyl groups act as electron mediators for the reduction of Fe^{3+}. The cathodic peak is the result of limited diffusion of Fe^{3+} from the solution bulk to the surface. When the potential of the modified electrode is scanned back to positive direction, ferrocene moiety is oxidized to ferricenium cations. However, since a part of ferrocenyl groups has been already oxidized to ferricenium cation by the Fe^{3+} in solution, the anodic current due to electrochemical oxidation of ferrocenyl groups is smaller than that without Fe^{3+} in solution. Moreover, the compact surface monolayer inhibits the direct electron transfer from Fe^{2+} to the electrode. Thus, the oxidation of Fe^{2+} in solution does not take place at the modified electrode. These results mean that $FcC_{11}SH$ modified electrode acts as a rectifier or a diode. This is a quite important property for constructing molecular electronic devices.

1.5.3 ELECTROCHEMICAL CHARACTERISTICS OF GOLD ELECTRODES MODIFIED WITH 2-(11-MERCAPTOUNDECYL)HYDROQUINONE (II)[24]

Figure 1.5.3 shows the cyclic voltammogram (CV) of gold electrode modified with 2-(11-mercaptoundecyl)hydroquinone ($H_2QC_{11}SH$, III), which has an alkyl chain of 11 carbon atoms, measured in 0.1 M $HClO_4$. A pair of redox peaks, corresponding to the oxidation of hydroquinone to benzoquinone and the reduction of benzoquinone to hydroquinone were observed at +490 mV and –90 mV, respectively. The peak separation observed at this electrode, 580 mV, is much larger than those observed at gold electrodes modified with 2-mercaptohydroquinone (H_2QSH : 40 mV),[24,25] which has no alkyl chains, and 2-(8-mercaptooctyl)hydroquinone (H_2QC_8SH : 240 mV),[26] which has an alkyl chain of 8 carbon atoms. These results clearly show that the electron transfer rate between the gold electrode and quinone group is strongly affected by the distance between the electrode and the redox active group in this case. This is in contrast to result observed at the gold electrodes modified with the self-assembled monolayer of ferrocenylalkanethiols.

The amount of saturated adsorption calculated from the CV was ca. 3.3×10^{14} molecules/cm^2, corresponding to one adsorbed $H_2QC_{11}SH$ molecule per 3.7 surface Au atoms. Hubbard *et al.* reported that the amounts of adsorption of 2,5-dihydroxy-4-methylbenzyl mercaptan ($H_2Q(CH_3)C_1SH$) and H_2QSH molecules on

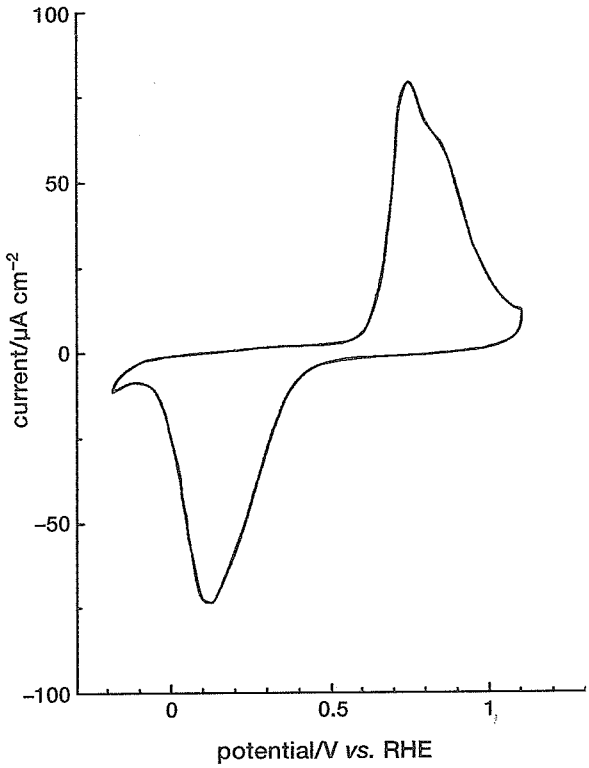

Figure 1.5.3. CV of the gold electrode modified with the $H_2QC_{11}SH$ SAM measured in 0.1 M $HClO_4$ with a scan rate of 100 mV/s.

a Pt(111) were 2.3×10^{14} and 1.6×10^{14} molecules/cm^2, respectively.[27] Their LEED study showed that the monolayer structure of the former was $2\sqrt{3} \times \sqrt{3}$ R30°. The amounts of adsorbed molecules on gold electrodes were H_2QSH [$(1.6 - 2.6) \times 10^{14}$ molecules/cm^2],[25,26,28] $H_2Q(CH_3)C_1SH$ [9.0×10^{13} molecules/cm^2][28] and H_2QC_8SH [$(1.8 - 3.0) \times 10^{14}$ molecules/cm^2].[6] The $H_2QC_{11}SH$ monolayer shows the highest amount of adsorption, indicating that the SAM of the $H_2QC_{11}SH$ on a gold surface is very well packed.

1.5.4 ELECTROCHEMICAL OXIDATION OF $C_2O_4^{2-}$ MEDIATED BY THE SAM OF $Ru(Bpy)_3^{2+}$-ALKANETHIOL DERIVATIVE (III) ON ITO AND ELECTROCHEMICAL LUMINESCENCE[29,30]

Figure 1.5.4 (a) shows the current-potential relations of the bare ITO (dotted line) and the (solid line) ITO electrode modified with $Ru(bpy)_3^{2+}$-alkanethiol $(Ru(bpy)_3^{2+}(C_{11}SH)_2$, III) in 0.4 M Na_2SO_4 solution containing 0.1 M $Na_2C_2O_4$ (pH = 4.7). At

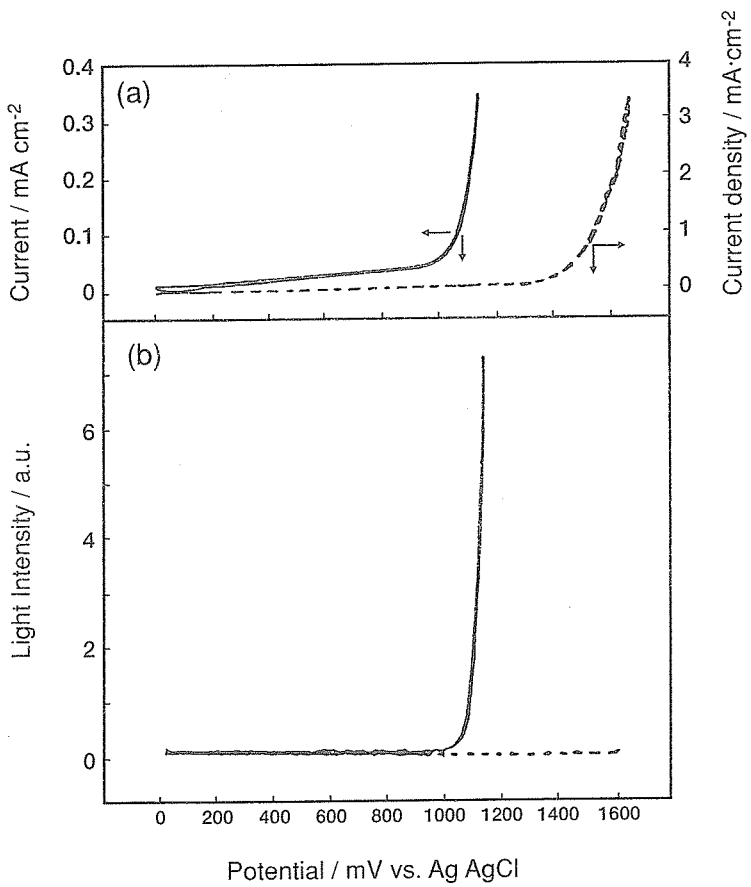

Figure 1.5.4. Potential dependence of (a) the currents of the unmodified (dotted line) and the $Ru(bpy)_3^{2+}(C_{11}SH)_2$ SAM modified (solid line) ITO electrodes and (b) the ECL intensity of the unmodified (dotted line) and the $Ru(bpy)_3^{2+}(C_{11}SH)_2$ SAM modified (solid line) ITO electrodes measured in a solution containing 0.4 M Na_2SO_4 and 0.1 M $Na_2C_2O_4$.

the bare ITO electrode, an anodic current started to flow around +1450 mV which is much more positive than the standard redox potential of oxalic acid, –555 mV (pH = 4.7). On the other hand, in the case of the $Ru(bpy)_3^{2+}(C_{11}SH)_2$ SAM modified ITO electrode, current started to increase at +1050 mV where the anodic current due to the oxidation of $Ru(bpy)_3^{2+}$ started to flow without $C_2O_4^{2-}$ in solution. This result suggests that the observed current is related to the oxidation of oxalate. Since the redox potential of $Ru(bpy)_3^{2+/3+}$ is more positive than the oxidation potential of oxalate, the $Ru(bpy)_3^{2+}$ group formed by anodic oxidation of $Ru(bpy)_3^{2+}$ can oxidize oxalate ion. Electrochemical luminescence (ECL) was observed at the potential region where anodic current flowed (Figure 1.5.4 (b), solid line). No emission was observed at the bare ITO electrode within the potential

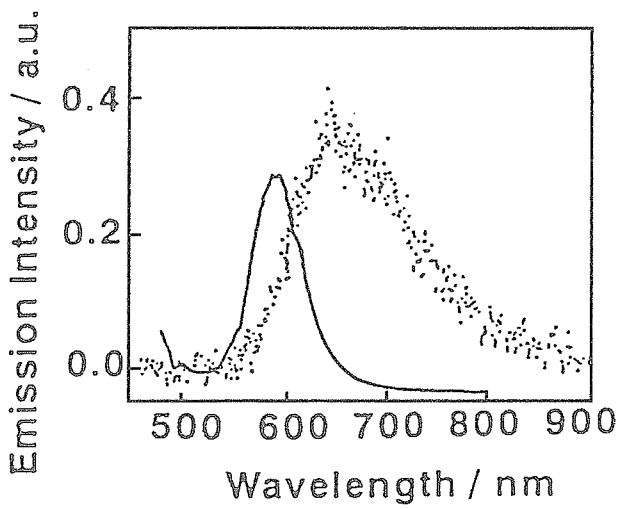

Figure 1.5.5. ECL spectrum of the $Ru(bpy)_3^{2+}(C_{11}SH)_2$ SAM modified ITO electrode in a solution containing 0.4 M Na_2SO_4 and 0.1 M $Na_2C_2O_4$ at +1150 mV (dots) and the emission spectrum of $Ru(bpy)_3^{2+}(C_{11}SH)_2$ in CH_2Cl_2 solution (solid line).

region investigated (Figure 1.5.4 (b), dotted line) even where anodic current was observed (Figure 1.5.4 (a), dotted line).

Figure 1.5.5 shows the emission spectrum of the $Ru(bpy)_3^{2+}(C_{11}SH)_2$ SAM modified ITO electrode obtained at +1150 mV (dots) in the same solution as mentioned above. A peak of the ECL spectrum is 650 nm which is close to the peak of $Ru(bpy)_3^{2+}$ dissolved in aqueous solution (610 nm),[31] suggesting the emission is from $Ru(bpy)_3^{2+*}$. In the case of ECL of $Ru(bpy)_3^{2+}$ in a solution containing $C_2O_4^{2-}$, $Ru(bpy)_3^{2+*}$ is assumed to be generated mainly by the reaction between $Ru(bpy)_3^{3+}$ and $Ru(bpy)_3^{+}$. In the present case, however, since the $Ru(bpy)_3^{2+}$ group is attached to the electrode surface and the potential is more positive than the redox potential of $Ru(bpy)_3^{2+/3+}$ and much more positive than that of $Ru(bpy)_3^{+/2+}$, it is very difficult to imagine the formation of $Ru(bpy)_3^{+}$ within the monolayer in this potential region. Therefore, these results indicate that the following processes take place in the anodic potential region where ECL is observed.

$$Ru(bpy)_3^{2+} \rightarrow Ru(bpy)_3^{3+} + e^- \quad (1.5.1)$$

$$Ru(bpy)_3^{3+} + C_2O_4^{2-} \rightarrow Ru(bpy)_3^{2+} + CO_2 + CO_2^{\bullet -} \quad (1.5.2)$$

$$Ru(bpy)_3^{3+} + CO_2^{\bullet -} \rightarrow Ru(bpy)_3^{2+*} + CO_2 \quad (1.5.3)$$

$$Ru(bpy)_3^{2+*} \rightarrow Ru(bpy)_3^{2+} + h\nu \quad (1.5.4)$$

$$Ru(bpy)_3^{2+*} \rightarrow Ru(bpy)_3^{3+} + e^- \quad (1.5.5)$$

In these processes, electrochemically generated $Ru(bpy)_3^{3+}$ oxidizes $C_2O_4^{2-}$, forming CO_2 and $CO_2^{\bullet-}$, and becomes $Ru(bpy)_3^{2+}$ which again donates an electron to the electrode (Eq. (1.5.1)). Thus, $Ru(bpy)_3^{2+/3+}$ head group of this monolayer on ITO electrode seems to act as a mediator for the oxidation of oxalate and therefore a monotonic increase in anodic current is observed as the potential becomes more positive. $CO_2^{\bullet-}$ reduces $Ru(bpy)_3^{3+}$ to $Ru(bpy)_3^{2+*}$ which has excess energy. $Ru(bpy)_3^{2+*}$ may donate an electron directly to the electrode (Eq. (1.5.5)) or relax to $Ru(bpy)_3^{2+}$ with light emission (Eq. (1.5.4)) which then donates the electron to the electrode (Eq. (1.5.1)). Thus, the emission efficiency is controlled by the electron transfer rate of reaction of Eq. (1.5.5) which should be dependent on the distance between the electrode and the $Ru(bpy)_3^{2+/3+}$ head group.

1.5.5 PHOTOINDUCED UP-HILL ELECTRON TRANSFER AT GOLD ELECTRODE MODIFIED WITH PORPHYRIN-MERCAPTOQUINONE (IV) AND PORPHYRIN-FERROCENE-THIOL (V) COUPLING MOLECULES[32–34]

UV, IR and X-ray photoelectron spectra of the gold modified with porphyrin-mercaptoquinone (PQSH, IV) and porphyrin-ferrocene-thiol ($PC_8FcC_{11}SH$, V) coupling molecules confirmed the chemisorption of this molecule on the gold surface.

For the PQSH SAM modified gold electrode,[32,33] in an electrolyte solution (pH = 4.5) containing methylviologen (MV^{2+}) as an electron acceptor and EDTA as an electron donor, anodic and cathodic photocurrents were observed at potentials more positive and more negative, respectively, than the redox potential of quinone moiety, +200 mV (Figure 1.5.6). In an electrolyte solution contains only EDTA, only anodic photocurrent was observed and only cathodic photocurrent was observed in an electrolyte solution containing MV^{2+} only. The action spectrum of the photocurrent was in good agreement with the absorption spectrum of porphyrin, indicating that the porphyrin group in the SAM acts as a photoactive site. These results indicate that the photoinduced electron transfer at the PQSH SAM takes place through the quinone moiety as schematically shown in Figure 1.5.6 as insets. If the electrode potential was more positive than the redox potential of quinone, photoexcited electron of porphyrin was transferred to the electrode through quinone group and electron transfer from EDTA to the vacant HOMO site of porphyrin took place. If the electrode potential was more negative than the redox potential of quinone, photoexcited electron of porphyrin was transferred to MV^{2+} and electron transfer from the electrode to the vacant HOMO site of porphyrin took place through quinone group.

The potential dependence of photocurrent shifted more negative as the pH became higher by 60 mV/pH. Critical potentials for the anodic/cathodic photocurrent transition at pH of 3.5, 4.5 and 5.5 were +260, +200 and +140 mV, respectively. These values were in good agreement with the redox potentials of the quinone moiety in the respective solutions. These results confirmed that the

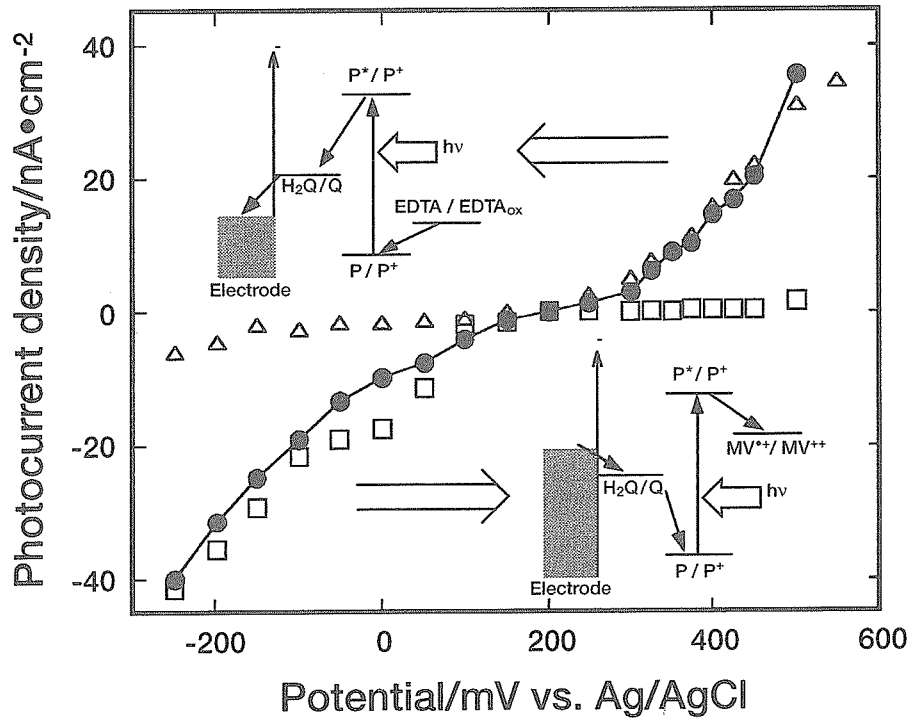

Figure 1.5.6. Potential dependence of the photocurrent at the gold electrode modified with the PQSH SAM. Solutions contain 0.1 M Na_2SO_4 (pH = 4.5) and (a) 50 mM EDTA and 5 mM MV^{2+} (closed circle), (b) 50 mM EDTA (open triangle) and (c) 5 mM MV^{2+} (open square). The insets illustrate the energy diagram of the electrode/electrolyte interface when the electrode potential was more positive (upper) or more negative (lower) than the redox potential of quinone moiety.

photoinduced electron transfer takes place through the quinone moiety and the direction of photoinduced electron transfer at the PQSH SAM modified gold electrode can be controlled by chemical species in the solution, electrode potential and pH of the solution.

Quantum efficiency of the PQSH SAM is, however, relatively low. This may be due to the fact that the PQSH molecule has no alkyl chains, the adsorbed amount of the molecules is low and, therefore, the orders of the molecular layers were low. In order to construct a more efficient electron transfer system, we designed and synthesized a novel molecule which has porphyrin, ferrocene and thiol groups as photoactive, electron transport or relay and surface binding groups, respectively, separated from each other by alkyl chains ($PC_8FcC_{11}SH$).[34] Ferrocene was chosen as the electron relay group because the electron transfer of this group is known to be very fast[35] and the alkyl chains were introduced to form a well-ordered SAM so that the reverse electron transfer and energy transfer from the excited porphyrin to the gold electrode can be reduced.

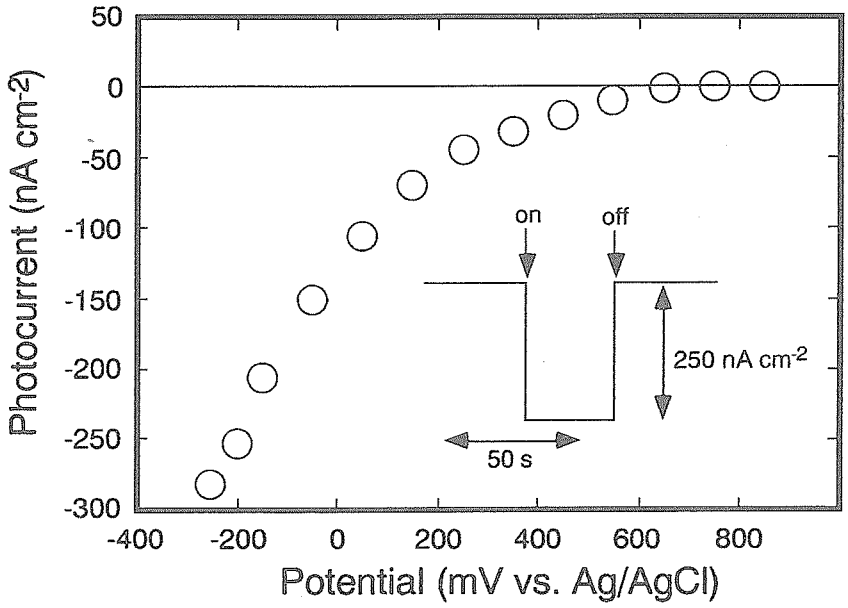

Figure 1.5.7. Potential dependence of photocurrent at the gold electrode modified with the $PC_8FcC_{11}SH$ SAM measured in the phosphate buffered 0.1 M $NaClO_4$ solution (pH = 4.5) containing 5 mM MV^{2+} as an electron acceptor when the electrode was illuminated with 430 nm pulsed light. Inset : Time course of the current at the $PC_8FcC_{11}SH$ SAM modified gold electrode held at –200 mV.

Photoelectrochemical characteristics of the $PC_8FcC_{11}SH$ SAM modified gold were investigated in a phosphate buffered 0.1 M $NaClO_4$ solution (pH = 4.5) containing 5 mM MV^{2+} as an electron acceptor. Inset of Figure 1.5.7 shows the time course of the current at –200 mV when the electrode was illuminated with 430 nm pulsed light. A stable cathodic photocurrent flowed as soon as the electrode was illuminated and fell instantly when illumination was terminated if the potential was more negative than +650 mV which coincides with the redox potential of the ferrocene moiety in the $PC_8FcC_{11}SH$ SAM (Figure 1.5.7). One should note that at the PQSH SAM modified gold, a cathodic photocurrent was observed only when the potential was more negative than +200 mV which is in agreement with the redox potential of the quinone moiety in the PQSH SAM and the photocurrent was much smaller, as mentioned above. The stable photocurrent flowed for more than 3 h without any signs of deterioration when the potential was kept between +650 and –250 mV. After prolonged illumination of the electrode, the color of the solution in front of the electrode changed to blue, showing that MV^{2+} was reduced to the methylviologen cation radical ($MV^{+\bullet}$).

Figure 1.5.8 shows an absorption spectrum of the $PC_8FcC_{11}SH$ SAM observed in air and a photocurrent action spectrum of the $PC_8FcC_{11}SH$ SAM modified gold electrode obtained at –200 mV. A strong peak at 430 nm and four small peaks between 500 and 700 nm were observed in the absorption spectrum. This spectrum

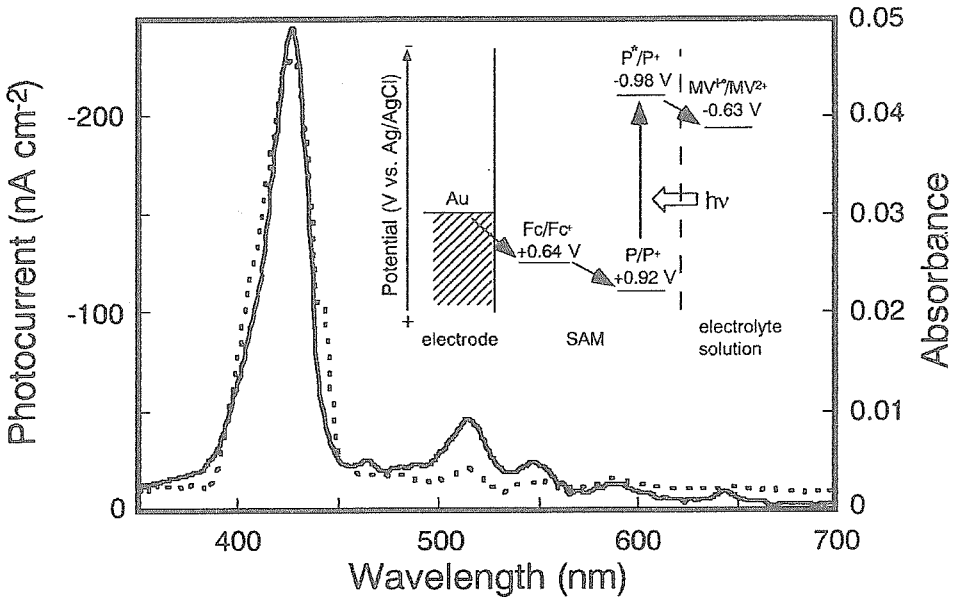

Figure 1.5.8. An absorption spectrum of the $PC_8FcC_{11}SH$ SAM on a transparent gold substrate observed in air (dotted line) and a photocurrent action spectrum of the $PC_8FcC_{11}SH$ modified gold electrode (solid line). Other conditions were as for Figure 1.5.7. Inset: Energy diagram for the $PC_8FcC_{11}SH$ modified gold electrode/MV^{2+} solution interface when the electrode potential is more negative than the redox potential of the ferrocene moiety. Fc, Fc^+, P, P^+ and P^* are ferrocene, ferricenium cation, porphyrin, oxidized state of porphyrin and excited state of porphyrin, respectively.

is similar to the absorption spectra of the same molecule and free-base porphyrin[36] in benzene solution. The strong peak at 430 nm and four small peaks can be assigned to the Soret band and the Q bands of the porphyrin ring, respectively. The Soret band of the SAM was red-shifted by ca. 10 nm from and was broader than that in solution, suggesting the existence of an interaction between the porphyrin rings in the SAM.[37] The shape of the photocurrent action spectrum is in very good agreement with the absorption spectrum of the SAM, confirming that the porphyrin group in the SAM really acted as a photoactive site.

Quantum efficiency based on the number of photons absorbed by the SAM was calculated by using the photocurrent and the absorbance determined from the absorption spectrum. When the electrode kept at –200 mV was illuminated by monochromated 430 nm light, the photocurrent density was 250 nA/cm^2 and the calculated quantum efficiency was 11%. The photoenergy conversion efficiency at this condition is calculated to be 1.8% as the input photon energy is 2.9 eV and the energy difference between the redox potential of $MV^{2+}/MV^{+\bullet}$ (–630 mV) and the electrode potential (–200 mV) is 0.43 eV. This is the highest quantum efficiency and energy conversion efficiency ever reported for photoinduced electron transfer at a monolayer modified metal electrode.[38–40]

1.5.6 CONCLUSION

The control of the electron transfer direction is achieved at gold and/or ITO electrodes modified with self-assembled monolayers (SAMs) containing various functional groups such as ferrocene, hydroquinone, porphyrin and $Ru(bpy)_3^{2+}$ groups. As the structure of molecular films on a metal and semiconductor substrates can be controlled by SA technique and thickness of the SAM is only 10–30 Å, ultra-micro molecular devices using the SA technique should be possible in the near future.

REFERENCES

1. Stryer, L. (1988). *Biochemistry*, 3rd Ed., Freeman, New York.
2. Ulman, A. (1991). *An Introduction to Ultrathin Organic Films from Langmuir-Blodgett to Self-Assembly*. New York: Academic Press.
3. Roberts, G. (1990). *Langmuir-Blodgett Films*. New York: Plenum Press.
4. Chidsey, C.E.D., Bertozzi, C.R., Putvinski, T.M. and Mujsce, A.M. (1990). *J. Am. Chem. Soc.*, **112**, 4301.
5. Walczak, M.M., Popenoe, D.D., Deinhammer, R.S., Lamp, B.D., Chung, C. and Porter, M.D. (1991). *Langmuir*, **7**, 2687.
6. Hickman, J.J., Ofer, D., Laibinis, P.E., Whitesides, G.M. and Wrighton, M.S. (1991). *Science*, **252**, 688.
7. Lee, K.A.B. (1990). *Langmuir*, **6**, 709.
8. Katz, E., Itzhak, N. and Willner, I. (1993). *Langmuir*, **9**, 1392.
9. Sasaki, T., Bae, I.T. and Scherson, D.A. (1990). *Langmuir*, **6**, 1234.
10. Obeng, Y.S. and Bard, A.J. (1991). *Langmuir*, **7**, 195.
11. Uosaki, K., Sato, Y. and Kita, H. (1991). *Langmuir*, **7**, 1510.
12. Uosaki, K., Sato, Y. and Kita, H. (1991). *Electrochim. Acta*, **36**, 1799.
13. Shimazu, K., Yagi, I., Sato, Y. and Uosaki, K. (1992). *Langmuir*, **8**, 1385.
14. Shogen, S., Kawasaki, M., Kondo, T., Sato, Y. and Uosaki, K. (1992). *Appl. Organometal. Chem.*, **6**, 533.
15. Ohtsuka, T., Sato, Y. and Uosaki, K. (1994). *Langmuir*, **10**, 3658.
16. Shimazu, K., Yagi, I., Sato, Y. and Uosaki, K. (1994). *J. Electroanal. Chem.*, **372**, 117.
17. Shimazu, K., Ye, S., Sato, Y. and Uosaki, K. (1994). *J. Electroanal. Chem.*, **375**, 409.
18. Sato, Y., Frey, B.L., Corn, R.M. and Uosaki, K. (1994). *Bull. Chem. Soc. Jpn.*, **67**, 21.
19. Sato, Y. and Uosaki, K. (1994). *Denki Kagaku*, **62**, 1269.
20. Kondo, T., Takechi, M., Sato, Y. and Uosaki, K. (1995). *J. Electroanal. Chem.*, **381**, 203.
21. Ye, S., Sato, Y. and Uosaki, K. (1997). *Langmuir*, **13**, 3157.
22. Yamada, R. and Uosaki, K. (1997). *Denki Kagaku*, **65**, 440.
23. Sato, Y., Itoigawa, H. and Uosaki, K. (1993). *Bull. Chem. Soc. Jpn.*, **66**, 1032.
24. Ye, S., Yashiro, A., Sato, Y. and Uosaki, K. (1996). *J. Chem. Soc., Faraday Trans.*, **92**, 3813.
25. Mebrau, T., Buttry, G.M., Bravo, B.G., Michelnaugh, S.L. and Soriaga, M.P. (1988). *Langmuir*, **4**, 1147.
26. Sato, Y., Fujita, M., Mizutani, F. and Uosaki, K. (1996). *J. Electroanal. Chem.*, **409**, 145.
27. Stern, D.A., Wellner, E., Salaita, G.N., Davidson, L.L., Lu, F., Frank, D.G., Zapien, D.C., Walton, N. and Hubbard, A.T. (1988). *J. Am. Chem. Soc.*, **110**, 4885.
28. Mo, Y., Sabdifer, M., Sukenik, C., Barriga, R.J., Soriag, M.P. and Scherson, D.A. (1995). *Langmuir*, **11**, 4626.
29. Sato, Y. and Uosaki, K. (1993). *Denki Kagaku*, **61**, 816.
30. Sato, Y. and Uosaki, K. (1995). *J. Electroanal. Chem.*, **384**, 57.
31. Zhang, X. and Bard, A.J. (1988). *J. Phys. Chem.*, **92**, 5566.
32. Kondo, T., Ito, T., Nomura, S. and Uosaki, K. (1996). *Thin Solid Films*, **284/285**, 652.
33. Kondo, T., Yanagida, M., Ito, T., Nomura, S. and Uosaki, K. (1997). *J. Electroanal. Chem.*, in press.
34. Uosaki, K., Kondo, T., Zhang, X.-Q. and Yanagida, M. (1997). *J. Am. Chem. Soc.*, **119**, 8367.
35. Chidsey, C.E.D. (1991). *Science*, **251**, 919.
36. Gouterman, M. (1978). *The Porphyrin*, edited by D. Dofphin, Vol. III. New York: Academic Press.

37. Zak, J., Yuan, H., Ho, M., Woo, L.K. and Porter, M.D. (1993). *Langmuir*, **9**, 2772.
38. Seta, P., Bienvenue, E., Moore, A.L., Mathis, P., Bensasson, R.V., Liddell, P., Pessiki, P.J., Joy, A. and Moore, T.A. (1985). *Nature*, **316**, 653.
39. Fujihira, M. (1990). *Mol. Cryst. Liq. Cryst.*, **183**, 59.
40. Akiyama, T., Imahori, H., Ajawakom, A. and Sakata, Y. (1996). *Chem. Lett.*, 907.